Research Article | Vol. 26, No. 10 | 14 May 2018 | OPTICS EXPRESS 12536
Optics EXPRESS

Cascaded interactions mediated by terahertz radiation

M. Hemmer,[1,5,*] G. Cirmi,[1,2,5] K. Ravi,[1,3,5] F. Reichert,[1] F. Ahr,[1,2] L. Zapata,[1] O. D. Mücke,[1,2] A.-L. Calendron,[1,2] H. Çankaya,[1,2] D. Schimpf,[1] N. H. Matlis,[1] and F. X. Kärtner[1,2,3,4]

[1]*Center for Free-Electron Laser Science, Deutsches Elektronen-Synchrotron DESY, Notkestraße 85, 22607 Hamburg, Germany*
[2]*The Hamburg Centre for Ultrafast Imaging, Luruper Chaussee 149, 22761 Hamburg, Germany*
[3]*Department of Electrical Engineering and Computer Science and Research Laboratory of Electronics, 77 Massachusetts Avenue, Massachusetts Institute of Technology, Cambridge, MA 02139, USA*
[4]*Physics Department, University of Hamburg, Luruper Chaussee 149, 22761 Hamburg, Germany*
[5]*These authors contributed equally*
**michael.hemmer@cfel.de*

Abstract: We investigate a regime of parametric amplification in which the pump and signal waves are spectrally separated by only a few hundreds of GHz frequency – therefore resulting in a sub-THz frequency idler wave. Operating in this regime we find an optical parametric amplifier (OPA) behavior which is highly dissimilar to conventional OPAs. In this regime, we observe multiple three-wave mixing processes occurring simultaneously which results in spectral cascading around the pump and signal wave. Via numerical simulations, we elucidate the processes at work and show that cascaded optical parametric amplification offers a pathway toward THz-wave generation beyond the Manly-Rowe limit and toward the generation of high-energy, sparse frequency-combs.

Published by The Optical Society under the terms of the Creative Commons Attribution 4.0 License. Further distribution of this work must maintain attribution to the author(s) and the published article's title, journal citation, and DOI.

OCIS codes: (230.6080) Sources; (320.7110) Ultrafast nonlinear optics; (260.3090) Infrared, far; (160.3730) Lithium niobate.

References and links

1. P. A. Franken, A. E. Hill, C. W. Peters, and G. Weinreich, "Generation of optical harmonics," Phys. Rev. Lett. **7**(4), 118 (1961).
2. T. Popmintchev, M. C. Chen, D. Popmintchev, P. Arpin, S. Brown, S. Ališauskas, G. Andriukaitis, T. Balčiunas, O. D. Mücke, A. Pugzlys, A. Baltuska, B. Shim, S. E. Schrauth, A. Gaeta, C. Hernández-García, L. Plaja, A. Becker, A. Jaron-Becker, M. M. Murnane, and H. C. Kapteyn, "Bright coherent ultrahigh harmonics in the keV X-ray regime from mid-infrared femtosecond lasers," Science **336**(6086), 1287–1291 (2012).
3. F. Silva, D. R. Austin, A. Thai, M. Baudisch, M. Hemmer, D. Faccio, A. Couairon, and J. Biegert, "Multi-octave supercontinuum generation from mid-infrared filamentation in a bulk crystal," Nat. Commun. **3**, 807 (2012).
4. P. B. Corkum, "Plasma Perspective on Strong Field Multiphoton Ionization," Phys. Rev. Lett. **71**(13), 1994–1997 (1993).
5. A. Couairon and A. Mysyrowicz, "Femtosecond filamentation in transparent media," Phys. Rep. **441**(2–4), 47–189 (2007).
6. J. A. Armstrong, N. Bloembergen, J. Ducuing, and P. S. Pershan, "Interactions between Light Waves in a Nonlinear Dielectric," Phys. Rev. **127**(6), 1918 (1962).
7. R. A. Baumgartner and R. L. Byer, "Optical parametric amplification," IEEE J. Quantum Electron. **15**(6), 432–444 (1979).
8. M. Cronin-Golomb, "Cascaded nonlinear difference-frequency generation of enhanced terahertz wave production," Opt. Lett. **29**(17), 2046–2048 (2004).
9. A. G. Stepanov, A. A. Mel'nikov, V. O. Kompanets, and S. V. Chekalin, "Spectral modification of femtosecond laser pulses in the process of highly efficient generation of terahertz radiation via optical rectification," JEPT Lett. **85**(5), 227–230 (2007).
10. A. Varanavičius, A. Dubietis, A. Berzanskis, R. Danielius, and A. Piskarskas, "Near-degenerate cascaded four-wave mixing in an optical parametric amplifier," Opt. Lett. **22**(21), 1603–1605 (1997).
11. D. Molter, M. Theuer, and R. Beigang, "Nanosecond terahertz optical parametric oscillator with a novel quasi phase matching scheme in lithium niobate," Opt. Express **17**(8), 6623–6628 (2009).

#320235 https://doi.org/10.1364/OE.26.012536
Journal © 2018 Received 22 Jan 2018; revised 21 Mar 2018; accepted 21 Mar 2018; published 2 May 2018

Optics EXPRESS

12. D. A. Walsh, P. G. Browne, M. H. Dunn, and C. F. Rae, "Intracavity parametric generation of nanosecond terahertz radiation using quasi-phase-matching," Opt. Express **18**(13), 13951–13963 (2010).
13. M. Bache, O. Bang, B. B. Zhou, J. Moses, and F. W. Wise, "Optical Cherenkov radiation in ultrafast cascaded second-harmonic generation," Phys. Rev. A **82**(6), 063806 (2010).
14. M. Bache, J. Moses, and F. W. Wise, "Scaling laws for soliton pulse compression by cascaded quadratic nonlinearities," J. Opt. Soc. Am. B **24**(10), 2752–2762 (2007).
15. I. Jovanovic, C. P. Barty, C. Haefner, and B. Wattellier, "Optical switching and contrast enhancement in intense laser systems by cascaded optical parametric amplification," Opt. Lett. **31**(6), 787–789 (2006).
16. E. A. Nanni, W. R. Huang, K. H. Hong, K. Ravi, A. Fallahi, G. Moriena, R. J. D. Miller, and F. X. Kärtner, "Terahertz-driven linear electron acceleration," Nat. Commun. **6**(1), 8486 (2015).
17. F. X. Kärtner, F. Ahr, A.-L. Calendron, H. Çankaya, S. Carbajo, G. Chang, G. Cirmi, K. Dörner, U. Dorda, A. Fallahi, A. Hartin, M. Hemmer, R. Hobbs, Y. Hua, W. R. Huang, R. Letrun, N. Matlis, V. Mazalova, O. D. Mücke, E. Nanni, W. Putnam, K. Ravi, F. Reichert, I. Sarrou, X. Wu, A. Yahaghi, H. Ye, L. Zapata, D. Zhang, C. Zhou, R. J. D. Miller, K. K. Berggren, H. Graafsma, A. Meents, R. W. Assmann, H. N. Chapman, and P. Fromme, "AXSIS: exploring the frontiers in attosecond X-ray science, imaging and spectroscopy," Nucl. Instruments Methods Phys. Res. Sect. A Accel. Spectrometers, Detect. Assoc. Equip. **829**, 24–29 (2016).
18. K. Ravi, M. Hemmer, G. Cirmi, F. Reichert, D. N. Schimpf, O. D. Mücke, and F. X. Kärtner, "Cascaded parametric amplification for highly efficient Terahertz generation," Opt. Lett. **41**(16), 3806–3809 (2016).
19. K. Ravi, D. N. Schimpf, and F. X. Kärtner, "Pulse sequences for efficient multi-cycle terahertz generation in periodically poled lithium niobate," Opt. Express **24**(22), 25582–25607 (2016).
20. G. Cirmi, M. Hemmer, K. Ravi, F. Reichert, L. E. Zapata, A.-L. Calendron, H. Cankaya, F. Ahr, O. D. Muecke, N. H. Matlis, and F. X. Kaertner, "Cascaded second-order processes for the efficient generation of narrowband terahertz radiation," J. Phys. At. Mol. Opt. Phys. **50**(4), 044002 (2017).
21. X. Wu, C. Zhou, W. R. Huang, F. Ahr, and F. X. Kärtner, "Temperature dependent refractive index and absorption coefficient of congruent lithium niobate crystals in the terahertz range," Opt. Express **23**(23), 29729–29737 (2015).
22. F. Ahr, S. W. Jolly, N. H. Matlis, S. Carbajo, T. Kroh, K. Ravi, D. N. Schimpf, J. Schulte, H. Ishizuki, T. Taira, A. R. Maier, and F. X. Kärtner, "Narrowband terahertz generation with chirped-and-delayed laser pulses in periodically poled lithium niobate," Opt. Lett. **42**(11), 2118–2121 (2017).

1. Introduction

Manipulating the frequency of electromagnetic fields is a major application of nonlinear optics [1]. The past fifty-six years have witnessed a steady increase in the understanding and exploitation of nonlinear optical interactions. As a result, sources of coherent radiation now exist that extend from the soft X-ray [2] to the terahertz (THz) region of the electromagnetic spectrum and sources spanning multiple octaves of bandwidth are routinely operated [3]. Reaching the soft X-ray spectral region has only been achieved via nonlinear interactions beyond the perturbative limit – such as high harmonic generation (HHG) [4, 5] and supercontinuum generation typically involves a simultaneous number of nonlinear processes. However, obtaining radiation from the VUV to terahertz frequencies is achieved using perturbative second-order type interactions of three waves at optical frequencies.

Three-wave mixing processes typically enable frequency up-conversion – via sum-frequency generation (SFG) – or frequency down-conversion – via difference-frequency generation (DFG). Each of these processes find other nomenclatures for various sets of initial conditions [6]: for instance SFG is called second harmonic generation (SHG) when two input fields with frequency difference in the vicinity of zero are present, DFG is dubbed optical rectification (OR) when two optical fields of similar or equal frequency are set as input; DFG is termed optical parametric amplification (OPA), when one of the lower frequency inputs is of significantly weaker strength compared to the highest frequency input and OPA becomes optical parametric generation (OPG) when only the highest frequency wave is injected into the nonlinear optical medium, while the signal and idler pulses are amplified from quantum noise. In principle, all these processes may be described by the same set of coupled differential equations that differ in initial conditions, in particular in relative field strengths or in frequencies of the three interacting waves [7]. In addition, the dynamics of spectral evolution for each set of initial conditions varies, often characterizing and typifying the behavior of the particular second-order nonlinear process at work.

In this work, we experimentally and theoretically investigate a set of initial conditions left mostly unexplored [8, 9] over the past fifty six years. This set consists of a series of lines of

Optics EXPRESS

arbitrary intensity in the near infra-red (NIR) spectral region that are separated by a constant sub-terahertz frequency offset. Within this general class of input formats, we investigate one which is identical to the conventional OPA.

We show via experiments – which are corroborated by simulations – that this OPA possesses a unique spectro-temporal behavior originating from the simultaneous evolution of a large number of strongly coupled, phase-matched, nonlinear second-order processes. The occurrence of such multi-wave mixing phenomena primarily stems from the relatively small separation in frequency of the input waves and is hence unique to the chosen terahertz frequency range. As a result, a number of unique behaviors are observed including: indifference to relative pump intensity (i.e pump can be of lower intensity than signal/seed), different behavior upon seeding at signal (NIR) or idler (THz) frequencies and reliance on gain medium dispersion for efficient OPA operation. These anomalies may occur even at zero optical-to-THz energy conversion efficiencies, thus obviating the widely deployed three-wave approximation for terahertz OPAs. In fact, the use of a three-wave model for these interactions has produced limited understanding of such multi-wave systems despite experimental signatures being briefly observed [10]. Here, we present a mechanistic understanding of the processes at work responsible for the various implications stated above.

Henceforth, we refer to this multi-wave mixing as cascading for the sake of brevity. However, one must distinguish this from prior usage of the term, which either arises in the context of many phase-mismatched second order nonlinearities [11–14] or in the sequential physical arrangement of OPA systems [15]. In our experiments, we show that the energy of the two input waves can be redistributed in up to ten cascaded orders by the concomitant evolution of a large number of phase-matched processes and investigate ways to manipulate experimental initial conditions to control the spectral evolution. Upon disentangling the mechanisms at play in these cascaded processes, we determine via numerical simulations, the conditions which bring the cascaded optical parametric amplification behavior into the familiar regime of exponential growth of terahertz power with the length of the nonlinear medium. Optimizing and tailoring this new regime of parametric amplification has implications for technologically relevant applications such as highly efficient multi-cycle terahertz field generation – with applications for e.g. terahertz-driven particle acceleration [16] and X-ray generation [17]. Furthermore, an experimental measurement of the temporal waveform of the modified NIR envelope depicts the formation of a train of pulses. This verifies the coherence of the multi-wave mixing process and makes this approach amenable for the generation of high-energy, sparse optical frequency combs.

2. Cascaded regime of optical parametric amplification for terahertz generation

We adopt the convention commonly employed to describe three-wave mixing processes naming the highest injected frequency wave (ω_p) the pump wave, the intermediate injected frequency wave (ω_s) the signal wave and the lowest (non-injected) frequency wave (ω_i) the idler wave ($\omega_p > \omega_s > \omega_i$). The interaction we investigate relies exclusively on an ensemble of three-wave mixing processes: we inject sub-nanometer linewidth pump (ω_p) and signal (ω_s) waves, separated by a sub-THz frequency (~nanometer wavelength separation) in a nonlinear medium optimized for phase-matched parametric amplification of the idler and signal waves (Fig. 1 – top).

Owing to the close spectral vicinity of the pump and signal waves, the generated idler wave can interact phase-matched via DFG with the signal wave and via phase-matched SFG with the pump wave to generate red and blue-shifted components, spectrally separated by the idler photon energy ($\hbar\omega_i$) from the signal pump waves respectively (Fig. 1 – middle). SFG between the idler and signal and DFG between the idler and pump can also occur phase-matched and result in back conversion into the pump and signal respectively. The process can then avalanche (or *cascade*) when the newly generated red- and blue-shifted spectral peaks interact similarly with the idler wave to generate the next set of red and blue-shifted spectral

Optics EXPRESS

components (Fig. 1 – bottom). The cascading process is eventually clamped either when the idler is damped by absorption or when the cascaded orders have extended beyond the phase-matching bandwidth of the gain medium. Notice that contrary to red-shifted peaks, the amplification of the blue-shifted spectral peaks consumes idler photons. As a consequence, the presence of dispersion – yielding a preferential red-shift in the case of the nonlinear crystal used in this study – is necessary to observe a net growth of the idler wave [18]. Furthermore, a number of additional energy transfers are also possible in this scheme that consist in energy back transfer into *e.g.* the pump and signal waves or into already existing cascaded peaks as illustrated in Fig. 1. All the aforementioned interactions tend to be very well phase-matched and strongly coupled, owing to the small value of THz frequencies. As a result, the initial input format is rapidly washed out and the pump energy undergoes significant spectral re-distribution. Therefore, it matters little if the pump frequency is of lower intensity than the signal, again contrary to conventional OPAs.

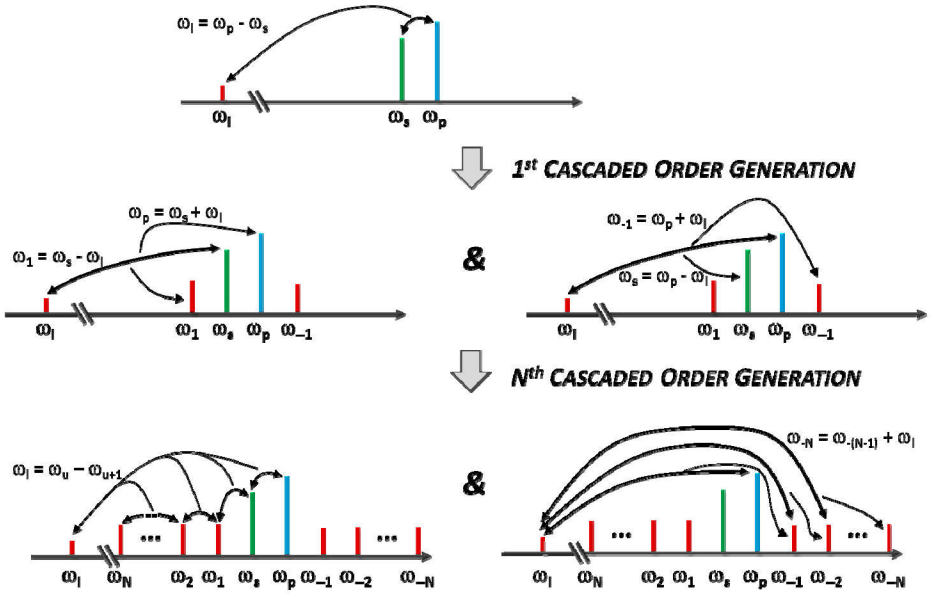

Fig. 1. Schematic representation of the multi-wave mixing or cascading process. (Top) Narrowband – single longitudinal mode to a few hundreds of picometers – pump (ω_p) and seed (ω_s) pulses with neighboring central frequency – in the nanometer to few nanometers range – in the optical domain are fed into a nonlinear medium. An idler wave (ω_i) in the terahertz frequency domain is generated via phase-matched three-wave mixing. (Middle) Upon generation of the idler wave (ω_i), the latter interacts with the signal wave (ω_s) to generate the first red-shifted cascaded order ($\omega_1 = \omega_s - \omega_i$) via DFG or to feed energy back into the pump wave ($\omega_p = \omega_i + \omega_s$) via SFG. Additionally, the idler wave (ω_i) interacts with the pump wave ($\omega_{-1} = \omega_p + \omega_i$) to generate a blue-shifted cascaded order. (Bottom) The process then avalanches to generate N red-shifted orders as each pair (ω_N, ω_{N+1}) contributes to enhancing the idler wave (ω_i) constituting a series of N OPAs. Simultaneously, the generated terahertz frequency idler wave interacts with each blue-shifted order to create/enhance the next blue-shifted peak via SFG. The idler wave can similarly interact with each red-shifted peak via DFG. Notice that all the interactions involved in the cascaded orders generation only involve three-wave ($\chi^{(2)}$) mixing processes.

An important outcome of the presented experiments is that upon tuning the cascading process toward preferential red-shifting – via methods that we detail in this paper and theoretically predicted [18] – we can generate a series of N-cascaded spectral peaks which act in pairs as a series of N *in situ* parametric amplifiers adding coherently to the generation of THz frequency radiation. This regime, which is referred to as terahertz- cascaded optical parametric amplification (THz-COPA) in this context, is accompanied by the more familiar

Optics EXPRESS

exponential growth of idler power w.r.t length and allows for optical-to-terahertz energy conversion efficiency – which is defined as the ratio between the THz output idler pulse energy and the NIR input pump pulse energy – to significantly exceed the Manley-Rowe limit. This opens a pathway toward efficient multi-cycle terahertz wave generation. However, it must be emphasized that this exponential growth akin to conventional OPA's is only coincidental and the use of three-wave approximations to design such systems is invalid due to the many simultaneous interactions involved.

3. Experimental setup, results and numerical simulations

The THz-COPA consists of a single nonlinear gain medium (Fig. 2). We chose periodically poled lithium niobate crystals with 5% MgO doping (MgO:PPLN) with a poling period of 212 μm, allowing phase-matching of a 0.5 THz frequency idler wave for pump and signal waves around 1 μm wavelength at 300 K. The available crystals differed in length with a selection of 2 cm, 1 cm and 0.5 cm long crystals. The pump fluence applied to the crystal was adjustable and capped at 2 J/cm^2 to prevent laser-induced damage to the nonlinear medium. The pump and signal beam showed a Gaussian intensity profile and the widths of both beams were identically set to 1.3 mm diameter at 1/e^2. The seed fluence impinging on the crystal was set to 34 mJ/cm^2. The wavelengths of the pump and signal waves were set to λ_p = 1029.45 nm (ν_p = 0.29412 PHz) and λ_s = 1031.2 nm (ν_s = 0.29092 PHz) respectively. The duration of the driving pulses was measured to be ~200 ps, the energy of the signal wave was set to 230 μJ and the energy of the pump pulses could be scaled up to 15 mJ. Notice that pump and signal waves were derived from a common oscillator before being amplified in separate amplifiers.

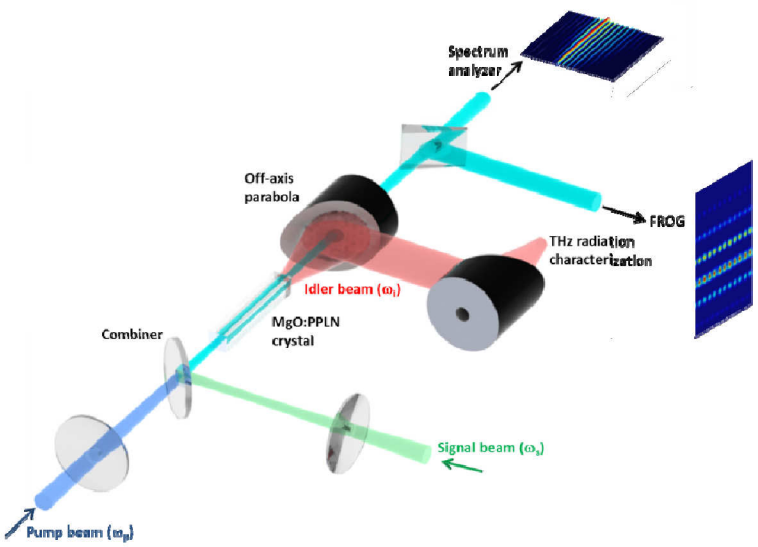

Fig. 2. Layout of the THz-COPA. Pump and seed beams were combined using a dielectric beam combiner and gently focused in an MgO:PPLN crystal with 212 μm poling period at room temperature. Detection setups include an optical spectral analyzer (OSA) with 0.1 nm resolution, a CCD camera used for relay imaging the end facet of the nonlinear medium (not shown) and a home-built SHG-FROG apparatus for temporal characterization of the pump and seed beams.

We performed spectral characterization using an optical spectrum analyzer (OSA) with a spectral resolution of 0.1 nm with ~50 dB dynamic range. Energy characterization of the idler wave in the THz regime was also performed: the THz radiation was collected at the output of the THz-COPA via a 2"-diameter, 10-cm focal length off-axis parabola equipped with a 3-mm diameter hole in the center to filter the high energy NIR waves (pump, signal and cascaded orders). A second, 2" diameter off-axis parabola focused the collected radiation onto

Optics EXPRESS

an energy detector calibrated for the terahertz frequency range. Additional plastic filters which were highly transparent at terahertz wavelengths and opaque at NIR wavelengths were placed in front of the detector to filter out residual NIR photons. The transmission of these plastic filters at THz wavelength was also calibrated. Energies in the NIR were measured using a pyroelectric power meter. The spatial intensity profiles of the overlapped NIR beams were constantly monitored under operation via relay imaging the end facet of the THz-COPA crystal using a CCD camera. The pump energy content lost to SHG for the 2 cm long crystal was estimated by recording the pump spectrum around 1030 nm for both the 0.5 cm and the 2 cm crystal and comparing the integrated value.

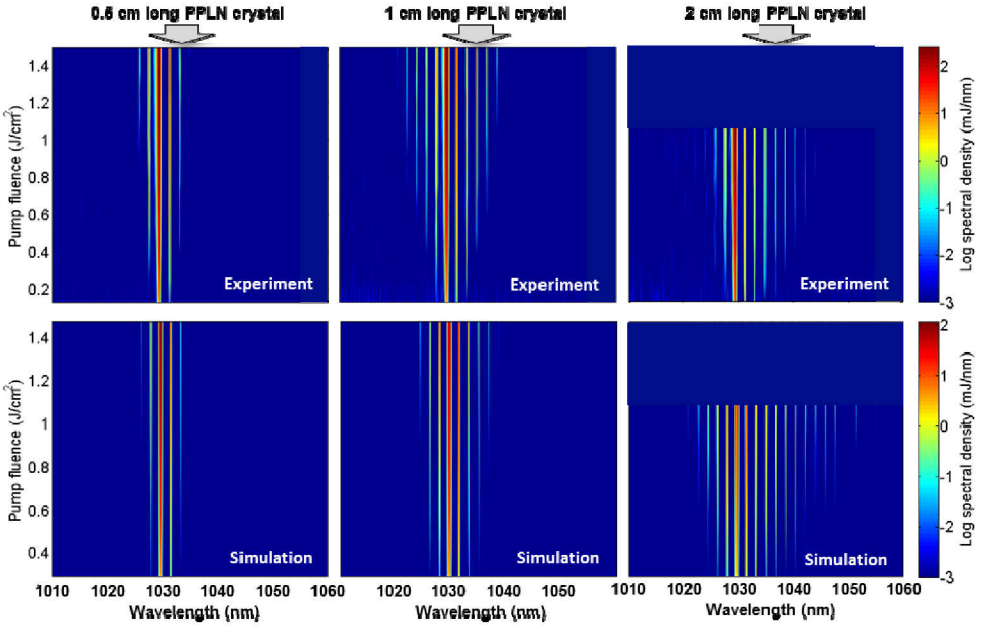

Fig. 3. (Upper row) Measured cascaded spectrum for in-band ($\Delta\lambda$ ~0.4 nm) seed energy at 1031.2 nm of ~230 μJ versus pump fluence in a 0.5 cm long MgO:PPLN crystal (left), 1 cm long MgO:PPLN crystal and (right) 2 cm long MgO:PPLN crystal; (lower row) Numerically simulated cascaded spectrum for in-band ($\Delta\lambda$ ~0.4 nm) seed energy at 1031.2 nm of ~230 μJ versus pump fluence in a 0.5 cm long MgO:PPLN crystal (left), 1 cm long MgO:PPLN crystal and (right) 2 cm long MgO:PPLN crystal. Notice that the maximum applied fluence on the 2 cm long sample was capped at 1.1 J/cm^2. The pump line is the strongest line located at 1029.5 nm for all plots, at all fluence levels.

For the experimental conditions described previously, we investigated the influence of crystal length and pump fluence on the cascading process (Fig. 3 – top row). A single red and blue-shifted peak with respect to the pump wavelength appear clearly above the noise floor for a modest pump fluence of ~0.6 J/cm^2 in a 0.5 cm long nonlinear gain medium as envisaged in Fig. 1 (middle). It is seen that increasing either the crystal length or the pump fluence further yields an increase in the number of cascaded spectral peaks (Fig. 3). Initially, the relative strength of blue and red-shifted peaks is roughly symmetric. However, this eventually gives way to preferential red-shifting. In particular, for a 2 cm long gain medium at a pump fluence of 1.1 J/cm^2, we observe the formation of up to eight red-shifted and four blue-shifted peaks with respect to the initial pump frequency. Increasing either the crystal length or the pump fluence yields a preferential red-shifting of the 'center of mass' of the cascaded spectrum. This preferential red-shifting is a spectral signature of the DFG process between the original signal wave and subsequent red-shifted peaks with the THz frequency idler wave being favored over the SFG process between the initial pump wave and the THz

Optics EXPRESS

frequency idler (Fig. 1) to generate subsequent blue-shifted peaks. The origin of this preferential red-shift is further discussed below and was predicted in our earlier theoretical work [18]. Notice that we limited the fluence applied to the 2 cm long crystal to 1.1 J/cm^2 due to experimental uncertainties in the fluence handling of this particular crystal.

Our experiment was setup to enable energy calibration of the measured spectra therefore providing access to the energy content of each spectral peak as a function of crystal length and pump fluence (Fig. 3). In the case of the shortest gain medium, the energy increase of each cascaded peak follows a linear evolution with fluence, both on the blue- and red-shifted side of the pump. For both the 1 cm and 2 cm long gain media, we observed that while all blue-shifted and the low order red-shifted spectral lines follow a linear growth, the evolution of the energy content of the higher order red-shifted peaks appears to clamp. We attribute this clamping of the cascading process to the strong absorption experienced by the terahertz radiation in the PPLN crystal at room temperature (6 cm^{-1}). This is reasonable since absorption of terahertz radiation inhibits further driving of the cascading process. The energy content per spectral line, however reaches several tens to hundreds of microjoules. Finally we estimate that up to 20% of the pump wave is lost to second-harmonic generation (SHG) for the 2 cm long crystal at ~1.0 J/cm^2 fluence, a parasitic process whose efficiency strongly depends on the poling period of the crystal.

In order to gain understanding of the complex dynamics of the process, we used numerical simulations to analyze the experimental data shown in Fig. 3. In addition to models from our earlier works [18–20], numerical simulations governing the spatio-temporal dynamics of the system in three spatial dimensions were developed specifically to understand the experiments in Fig. 3. Numerical simulations which consider pump depletion by accounting for the coupled nonlinear interaction of the optical, terahertz and second harmonic pulses were utilized. The nonlinear interactions considered included second (DFG, SFG, SHG) and third order effects (instantaneous Kerr nonlinearities). Stimulated Raman scattering were found to minimally influence the results due to the resonances being far from 0.5 THz and were hence excluded in our simulations. Since the system is well approximated by conditions of radial symmetry, a (2 + 1)-D model spanning the radial (r), longitudinal (z) and temporal (t) dimensions was employed. The numerical method involved a split-step Hankel (for space-momentum)-Fourier (for time-frequency) transform, fourth-order Runge-Kutta scheme. The theoretical results show qualitative and quantitative agreement with the experimental results (Fig. 3 – top and bottom row).

The numerical simulation offers the freedom to access the gain medium properties, in particular its dispersion, which enabled us to elucidate the mechanism resulting in preferential red-shifting observed experimentally. Contrary to conventional OPAs, in the case of the THz-COPA, both the SFG and DFG processes are well phase-matched. Therefore, in the complete absence of dispersion, both processes occur at similar rates, leading only to modulation of the pump as well as terahertz power, which produces symmetric sidebands with respect to the pump wavelength. However, since most materials are dispersive, the phase-matching for either SFG or DFG processes is slightly preferred relative to the other. Therefore, in general after initial symmetric spectral broadening reminiscent of self-phase modulation via cascaded $\chi^{(2)}$, the spectral bandwidth reaches a domain where asymmetry in phase-matching influences the dynamics. At this point, one of the processes begins to dominate. In the case of PPLN, DFG processes are better phase-matched at ~1 μm wavelength. Therefore, after initial symmetric broadening, a preferential red-shift of the optical spectrum ensues at larger spectral bandwidths. Entering this regime of asymmetry may be hastened by increasing the pump fluence, seed levels, interaction length or by reducing the absorption of the terahertz wave. Alternatively, dispersion may be introduced by engineering the gain medium or the experimental conditions. From an experimental standpoint, readily accessible parameters are the pump fluence, signal levels, crystal lengths and crystal temperature.

Optics EXPRESS

We also experimentally measured the energy yield of the terahertz wave and obtained up to 160 nJ of energy at 0.5 THz frequency for a maximum pump fluence of 1.5 J/cm^2 using the 1 cm long PPLN crystal (Fig. 4). This results in a modest pump to idler efficiency – below the Manley-Rowe limit – of 1.6x10^{-5}. However, it is important to note is that despite such low conversion efficiency, undepleted approximations commonly employed for conventional OPA's are not valid in the case of the THz-COPA. This is clearly evident from the previously depicted spectral dynamics, which can only be explained by consideration the simultaneous evolution of several second order processes. We observe a linear dependency of the terahertz wave energy yield with signal energy (Fig. 4 – left) as well as a linear dependency with pump fluence (Fig. 4 – right). In addition, we observe that increasing the crystal length from 0.5 cm to 1 cm results in a marginal increase of ~20% in generated terahertz radiation. Certainly this is in line with the increasing degree of spectral asymmetry between red and blue-shifted peaks observed in Fig. 3. Further increasing the crystal length to 2 cm provides no further improvement in terahertz radiation yield. Both the spectral behavior and the THz yield are reproducible on a day-to-day basis and were only limited by the stability of the driving laser, similarly to a more standard OPA.

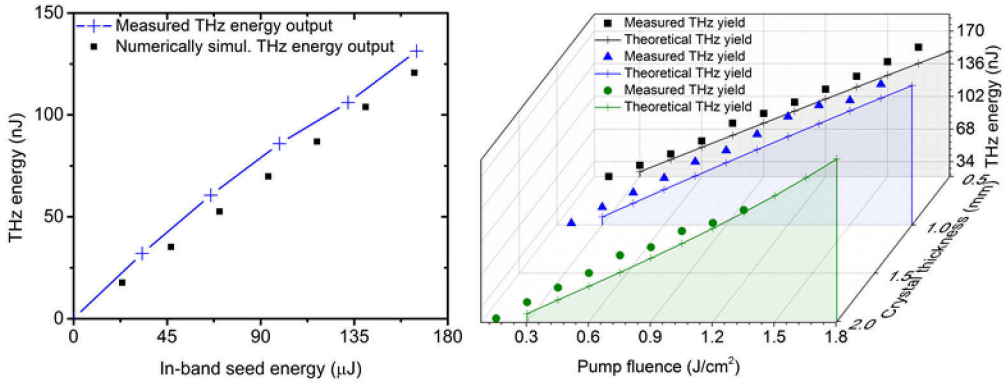

Fig. 4. (Left) Measured (blue line) and numerically simulated (black squares) THz radiation yield versus signal energy for the 1 cm long crystal and 1.5 J/cm^2 pump fluence and (right) versus pump fluence for the three crystals under consideration for a seed energy of 165 μJ.

We again resort to numerical simulations to understand the process negatively impacting the buildup of terahertz radiation. We first verify the accuracy of the model by numerically reproducing the experimental terahertz pulse energy presented in Fig. 4 and find good agreement between our experimental and numerical data (Fig. 4).We find that the rollover of terahertz energy with respect to crystal length is due to the absorption of terahertz radiation in the gain medium and conclude that for crystal lengths exceeding ~0.5 cm the terahertz yield clamps, limited by both the maximum fluence tolerated by the gain medium and the linear absorption of the terahertz wave.

We investigate the effect of reducing the terahertz absorption, by simulating the system at cryogenic temperatures of 100 K. The absorption coefficient reduces from ~6 cm^{-1} to ~2 cm^{-1} for lithium niobate [21] at a frequency of 0.5 THz frequency. The large time bandwidth product involved in these simulations leads to a heavy computational load. Therefore, we resort to a 1 + 1-D – simulation – i.e. only z propagation and time (or frequency) – code. We verified that it matches with the (2 + 1)-D code used above after accounting for spatial averaging effects. The numerical simulation reveals that while maintaining all other parameters identical, this results in a dramatic increase in the red-shifting of the NIR spectrum and commensurate increase in terahertz energy yield (Fig. 5). In particular, the maximum spectral extent of the cascading spectrum could span up to 200 nm of bandwidth extending from 1000 nm to 1200 nm at the plane of maximum intensity at cryogenic temperature as compared to ~75 nm at room temperature with a less pronounced red-shift

Optics EXPRESS

(Fig. – left). This spectral red-shift immediately translates into a gain in efficiency: for a 2 cm-long crystal, the conversion efficiency increases from our measured $1.6\text{x}10^{-5}$ at room temperature to $7\text{x}10^{-4}$ at 100 K temperature. It is worth reiterating that Fig. 5 plots spectra at point of maximum intensity in the transverse dimension as opposed to the spatially averaged spectra (over three spatial dimensions) in Fig. 3, which explains their larger spectral extent. In addition, with lower absorption, crystal lengths much greater than 0.5 cm can be used, significantly increasing the conversion efficiency. Put another way, the dramatic red-shifting is accompanied by the more familiar exponential growth of terahertz energy w.r.t length, akin to conventional OPA's.

Our simulation shows that efficiencies in the 1% range can be reached at cryogenic temperature when using a 4 cm long crystal. We also observe a rollover in the conversion efficiency as a function of pump fluence in the particular case of a 4 cm long cryogenically cooled crystal. We could numerically track the origin of this rollover to parasitic second harmonic generation of the pump. Finally, the numerical simulations confirm that the terahertz radiation from the THz-COPA is of high spectral brightness. It is dominantly generated at the terahertz frequency that corresponds to the fundamental periodicity of the PPLN. While harmonics (3^{rf}, 5th *etc*...) of this THz frequency are also phase-matched during the process, our computations show that these channels of energy transfer are intrinsically inefficient due to (*i*) the lower Fourier coefficients for higher order phase-matching, (*ii*) higher absorption at higher THz frequencies, and (*iii*) reduced number of NIR lines that can contribute to their nonlinear generation. The energy content of the harmonics compared to that of the fundamental THz frequency is lower by at least 20 dB.

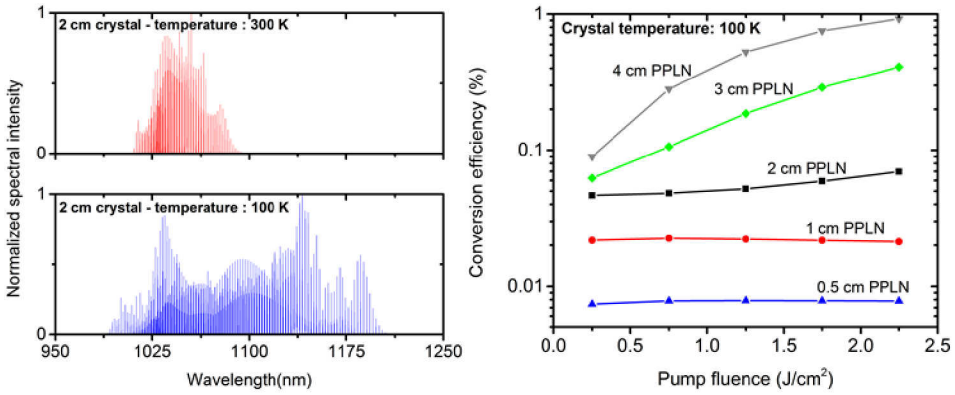

Fig. 5. (Left) Numerically simulated cascaded spectra plotted at the plane of maximum intensity (using 1 + 1-D) using pump and signal input parameters matching those of Fig. 3 for a crystal at room temperature (top) and a cryogenically cooled crystal (bottom); (right) computed conversion efficiency for various crystal length as a function of pump fluence for a crystal maintained at cryogenic temperature.

In summary, for a fluence set close to the damage fluence of the crystal, increasing the crystal length at room temperature results in increased cascading but no improvement on THz yield since idler absorption clamps the conversion efficiency to the 10^{-5} range. Reducing the idler absorption via cryogenic cooling enables making use of the full length of the crystal resulting in a clearly exponential growth, drastic red-shifting of the cascaded spectrum and ultimately conversion efficiencies in the 1% level.

Finally, the temporal structure of the NIR signal beam at the output of the THz-COPA is also of interest to gain insight into the coherence of the generation process and for frequency comb applications. The successive spectral peaks generated during the cascading process are expected to share a fixed phase relationship as the phase of the signal is transferred to each spectral peak – or comb tooth – via the terahertz wave. In the first OPA step as depicted in Fig. 1 (top), the phase coherent pump and seed wave derived from a common oscillator in our

Optics EXPRESS

setup interact and generate a terahertz frequency wave with stable carrier-envelope phase and zero carrier-envelope offset. The first red-shifted peak is obtained via DFG between the signal wave and the terahertz idler wave and therefore the phase of the signal is carried over to this spectral peak. Through the cascading process, the same phase is carried over to every red-shifted peak. Similarly, on the blue-shifted side of the spectrum, the first peak is obtained via SFG between the pump wave and the terahertz idler wave, resulting in a carrying-over of the phase of the pump wave. The pump itself is phase correlated to the signal wave, since pump and signal are derived from a common oscillator in our experiment. Such conservation of the phase guarantees a fixed phase relationship between all spectral peaks. The resulting spectrum therefore resembles that of a mode-locked oscillator operating at a 0.5 THz repetition rate. The phase-locking of the spectral modes was experimentally verified by measuring the temporal intensity of the cascaded signal wave at the output of the THz-COPA using second-harmonic generation frequency resolved optical gating (SHG-FROG) (Fig. 6 – top). The pump and signal waves were spectrally separated using a narrowband notch filter centered around the pump wavelength. The retrieved intensity profile of the signal wave at the output of the THz-COPA setup (Fig. 6 – bottom) shows pronounced modulation – resembling a pulse train – with 2 ps period (500 GHz frequency spacing), providing an experimental confirmation of the frequency-comb structure of the signal beam exiting the THz-COPA and the coherence of the process. The modulation in the temporal domain directly follows from the coherence of the process and the Fourier transformation of the cascaded spectrum into the temporal domain. The energy content per comb tooth is in the tens to hundreds of microjoules. The obtained pulse train is bound by the ~200 ps envelope of the original signal pulse. While the few picosecond pulses forming the 500 GHz pulse train are spectrally chirped, the spectral content of these pulses supports sub-ps duration. Further optimization of the OPA process – using *e.g.,* cryogenic cooling and longer gain media than those used in our experiment – could provide pulses in the 100 fs to sub-100 fs duration range.

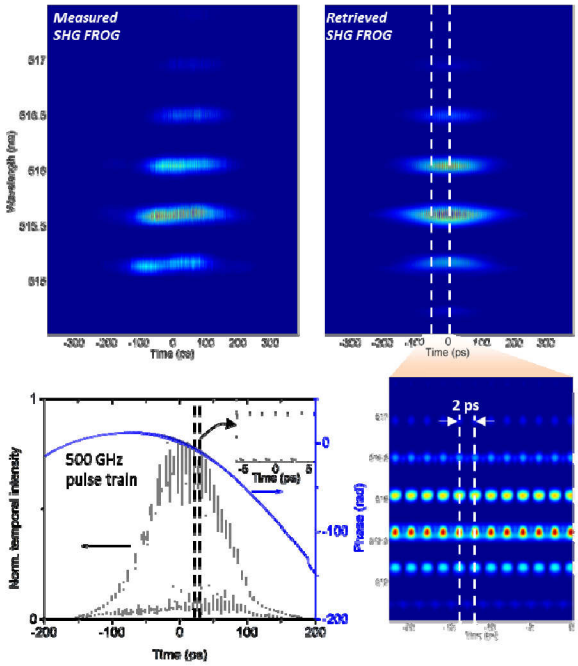

Fig. 6. (Top left) Measured SHG-FROG trace, obtained from the THz-COPA output after filtering the pump; (Top right) retrieved FROG trace; (bottom left) Retrieved temporal profile

Optics EXPRESS

and phase of the pulses from FROG; (bottom right) zoom of the retrieved FROG trace showing a strong modulation in time with 2-ps (1/0.5THz) period.

4. Conclusion

We have performed the first experiments, which provide a mechanistic understanding of the complex interplay between various phase-matched second order processes for OPA-like inputs with terahertz idler frequencies. The spectral dynamics investigated in these experiments illustrate the inefficacy of routinely used three-wave approximations of OPA's in the terahertz region and delineate methods to enter the regime of terahertz cascaded optical parametric amplification (THz-COPA). This approach promises to boost the optical-to-terahertz conversion efficiency of narrowband coherent radiation by orders of magnitude from the current state-of-the-art [20, 22]. We performed the experiments at room temperature and compared the results with simulations. The behavior in time of the NIR output makes it a potential source of high peak-power NIR pulse trains at high repetition rate. On the other hand, the terahertz output, with optimized temperature and crystal parameters, is a good candidate for achieving the high power, coherent, multi-cycle terahertz radiation in demand for electron acceleration to drive table-top FELs [17].

Funding

Helmholtz Association through DESY and the Center for Free-Electron Laser Science; European Research Council under the European Union's Seventh Framework Programme (FP/2007-2013) / ERC Grant Agreement n. 609920; Cluster of Excellence: The Hamburg Centre for Ultrafast Imaging-Structure, Dynamics and Control of Matter at the Atomic Scale of the Deutsche Forschungsgemeinschaft; Dr. Calendron acknowledges support from the Helmholtz Post-doctoral grant.

Acknowledgments

The authors also acknowledge Jan Schulte's contribution for early numerical computations.